JTTEE5 25:684–693
DOI: 10.1007/s11666-016-0399-3
1059-9630/$19.00 © ASM International

Accuracy of Young's Modulus of Thermal Barrier Coating Layer Determined by Bending Resonance of a Multilayered Specimen

Hiroyuki Waki, Kensuke Takizawa, Masahiko Kato, and Satoru Takahashi

(Submitted December 14, 2015; in revised form February 16, 2016)

The Young's modulus of individual layer in thermal barrier coating (TBC) system is an important mechanical property because it allows determining the parameters of materials mechanics in the TBC system. In this study, we investigated the accuracy of the evaluation method for the Young's modulus of a TBC layer according to the first bending resonance of a multilayered specimen comprising a substrate, bond coating, and TBC. First, we derived a closed-form solution for the Young's modulus of the TBC layer using the equation of motion for the bending vibration of a composite beam. The solution for the three-layered model provided the Young's modulus of the TBC layer according to the measured resonance frequency and the known values for the dimensions, mass, and Young's moduli of all the other layers. Next, we analyzed the sensitivity of these input errors to the evaluated Young's modulus and revealed the important inputs for accurate evaluation. Finally, we experimentally confirmed that the Young's modulus of the TBC layer was obtained accurately by the developed method.

Keywords composite beam, elastic modulus, MCrAlY, resonance, thermal barrier coating, yttria-stabilized zirconia

1. Introduction

Thermal barrier coatings (TBCs) are used for protecting the hot sections of gas-turbine engines and jet engines in order to lower the temperature of the underlying superalloy substrate. The TBC system consists of the TBC, a MCrAlY (M: Co and/or Ni) bond coating (BC), and the superalloy substrate. The TBC typically comprises yttria-stabilized zirconia and is deposited by thermal spraying. The MCrAlY coating is a protective coating that is used to protect the substrate from high-temperature oxidation and corrosion. The development of new materials and processes for high-performance coatings has been promoted because increasing the temperature of the turbine inlet enhances the thermal efficiency of the engines. For example, EB-PVD TBC with a columnar structure (Ref 1, 2) and segmented TBC with vertical cracks (Ref 3, 4) have been developed for the improvement of the turbine lifetime by relaxing the in-plane thermal stress. Furthermore, new processes (Ref 5, 6) for noble microstructures have been developed.

The Young's modulus of individual layer in TBC system is an important mechanical property because it allows determining the parameters of materials mechanics in the system, such as the thermal stress, residual stress, and interfacial fracture toughness. The calculation of Young's modulus from a freestanding TBC is easier than that from a TBC system. However, it is difficult to extract freestanding TBCs from columnar and segmented TBC systems, which have recently become important. Thus, the development of a determination method for the Young's modulus of the TBC layer using a TBC system specimen is essential.

The techniques used to measure the Young's modulus of TBC layer can be classified into three: mechanical-loading, resonance, and pulse-echo methods. The mechanical-loading methods are the most basic and are based on the direct measurement of the deformation resistance of the test material. For a TBC system specimen, the bending test is easy to perform and useful (Ref 7-11). On the contrary, the tensile test is difficult for an asymmetric specimen because of residual stress. Indentation tests (Ref 12, 13) which are one of the mechanical-loading methods, are also applicable to TBC system specimens. However, the obtained modulus is the value of

Hiroyuki Waki, Department of Mechanical Engineering, Iwate University, 4-3-5 Ueda, Morioka, Iwate 020-8551, Japan; **Kensuke Takizawa**, Graduate School of Engineering, Iwate University, 4-3-5 Ueda, Morioka, Iwate 020-8551, Japan; **Masahiko Kato**, Department of Mechanical System Engineering, Hiroshima University, 1-4-1 Kagamiyama, Higashi-Hiroshima, Hiroshima 739-8527, Japan; and **Satoru Takahashi**, Department of Mechanical Engineering, Tokyo Metropolitan University, 1-1 Minami-Osawa, Hachioji, Tokyo 192-0397, Japan. Contact e-mail: waki@iwate-u.ac.jp.

local area and depends on the magnitude of the indentation load. The pulse-echo method is based on the principle that the velocity of sound in a material depends on the elastic modulus of the material. This method has applications to TBC system specimens (Ref 14, 15). However, using this method, the evaluation of the in-plane Young's modulus, which is important for stress calculation, is generally difficult. The resonance method is based on the principle that the resonance frequency of a material depends on its elastic modulus. This method has few applications to TBC system specimens (Ref 16, 17) because the TBC system consists of three materials: TBC, BC, and substrate. There has been no analytical model of a three-layered system for the Young's modulus of the TBC top coating (TC). Determining a resonance frequency is easier and can be done more accurately than determining a deformation resistance. If the resonance method is expanded to a three-layered specimen, it will become a powerful technique.

In this study, we derived a closed-form equation for determining the Young's modulus of TBC layer in a TBC system specimen. The Young's modulus and thickness of the TBC layer are generally approximately one order of magnitude lower than those of the substrate. Consequently, the Young's modulus of the TBC layer for a multilayered specimen is considerably sensitive to experimental errors. This causes a large error in the obtained Young's modulus. Therefore, we investigated the determination accuracy analytically and revealed the important inputs for accurate evaluation. Finally, we experimentally investigated the accuracy of the method for some typical TBCs and showed its effectiveness.

2. Evaluation Method for the Young's Moduli of the Coatings Using the Bending Resonance of a Multilayered Specimen

2.1 Single-Layer Specimen

According to the dynamic beam vibration theory, without shear deflection and rotary inertia, the deflection $W(x, t)$ and resonance frequency f are expressed by Eq 1 and 2, respectively. The constant β is determined by boundary condition, and $\beta = 4.730$ for the first-mode vibration with free ends (Ref 18).

$$EI\frac{\partial^4 W}{\partial x^4} + \rho A\frac{\partial^2 W}{\partial t^2} = 0 \qquad \text{(Eq 1)}$$

$$f = \frac{\beta^2}{2\pi L^2}\left(\frac{EI}{\rho A}\right)^{\frac{1}{2}}, \qquad \text{(Eq 2)}$$

where E, I, ρ, A, and L are the Young's modulus, moment of inertia of area, density, sectional area, and length. The deflection W is expressed by a trigonometric function and hyperbolic function. The node is located $0.224L$ from the ends of the specimen, as shown in Fig. 1. The equation for

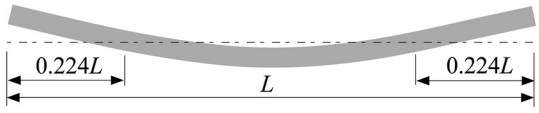

Fig. 1 First modal shape of free bending vibration of a beam

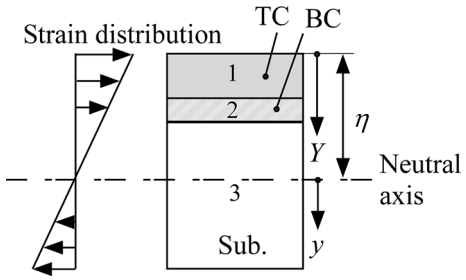

Fig. 2 Composite beam of the three-layered model consists of the substrate, BC, and TC

determining the Young's modulus can be derived from Eq 2. For the single-layer specimen, the equation for determining the Young's modulus is defined by ISO 17561:2002*, as shown in Eq 3, on the basis of Eq 2.

$$E = 0.9465 \times \frac{M \cdot f^2}{b} \times \left(\frac{L}{h}\right)^3 \times \left[1 + 6.585\left(\frac{h}{L}\right)^2\right]. \qquad \text{(Eq 3)}$$

Here, $M = \rho bhL$ is the mass of the specimen, and b and h represent the width and thickness, respectively. The coefficient 0.9465 is derived from $4\pi^2 \times 12/\beta^4$, and $[1 + 6.585(h/L)^2]$ is the approximate correction factor (≈ 1) for the effects of the shear deformation and rotary inertia.

2.2 Multilayered Specimen

Chiu et al. (Ref 19) proposed the following bilayer model without the correction factor for the effects of the shear deformation and rotary inertia using the composite-beam theory:

$$f = \frac{\beta^2}{2\pi L^2}\left(\frac{\sum_i E_i I_i}{\sum_i \rho_i A_i}\right)^{\frac{1}{2}}. \qquad \text{(Eq 4)}$$

The subscript term i represents the ith layer, where $i = 1, 2$ in the case of the bilayer model. We proposed a three-layered model comprising a TC, BC, and substrate, as shown in Fig. 2. Here, y is the distance from the neutral axis, as shown in Fig. 2; η is the distance of the neutral axis from the top surface; and Y is the distance from the top surface, as shown in Fig. 2. The η is given by the Young's modulus of the TC, and the moment of inertia of area I includes η. By substituting Eq 5 into Eq 4, we derive a closed-form equation for the Young's modulus of the TC, as shown in Eq 6.

*Fine ceramics (advanced ceramics, advanced technical ceramics)—test method for elastic moduli of monolithic ceramics at room temperature by sonic resonance, ISO 17561:2002.

$$\eta = \frac{\sum_{i=1}^{3} E_i \int_{A_i} Y dA_i}{\sum_{i=1}^{3} E_i A_i}, \quad I_i = \int_{A_i} y^2 dA_i \qquad \text{(Eq 5)}$$

$$E_c = \frac{-B + \sqrt{B^2 - 4AC}}{2A} \qquad \text{(Eq 6)}$$

$$A = \beta^4 h_c^4$$

$$B = 2h_c\left[\begin{array}{l}\beta^4\left[E_b h_b\left(2h_c^2 + 3h_c h_b + 2h_b^2\right) + E_s h_s\left\{2h_c^2 + 3h_c h_s + 6h_b^2 + 6h_b(h_c + h_s) + 2h_s^2\right\}\right] \\ \quad -24\pi^2 f^2 m L^3/b\end{array}\right]$$

$$C = \beta^4\left\{E_b^2 h_b^4 + 2E_b E_s h_b h_s\left(2h_b^2 + 3h_b h_s + 2h_s^2\right) + E_s^2 h_s^4\right\} - 48\pi^2 f^2 m L^3(E_b h_b + E_s h_s)/b$$

$$m = bL(h_c\rho_c + h_b\rho_b + h_s\rho_s)$$

$$\beta = 4.730.$$

Here, b and h represent the width and thickness, respectively. The subscripts "c," "b," and "s" represent the ceramic TC, the BC, and the substrate, respectively. The variable m represents the mass of the specimen and is expressed by the density of each layer. The Young's modulus of the TC can be obtained from the resonance frequency f of the TBC system specimen, if the dimensions and mass of the specimen and the Young's moduli of all the other layers are known. The calculation does not require the density of each layer but rather the mass of the specimen, which is easy to measure. Equation 6 does not consider the effects of the shear deformation and rotary inertia; therefore, we should select a slender specimen: $(h_s + h_b + h_c)/L \ll 1$.

The equations for determining the BC Young's modulus using a BC system specimen comprising a BC and a substrate are also derived from Eq 6, with the subscript "c" replaced by "b" after setting $h_b = 0$. The equations for determining the substrate Young's modulus using a substrate specimen are also derived from Eq 6, with the subscript "c" replaced by "s" after setting $h_b = 0$ and $h_s = 0$. The equation is identical to Eq 3 with a correction factor of 1.

Further, Eq 6 can be converted for determining the Young's modulus of any layer. The Young's modulus of any unknown layer of the system can be determined, if the dimensions and mass of the specimen and moduli of all the other layers are known.

3. Sensitivity of the TBC System Model to Errors

As shown in section 2.2, the Young's modulus of the TC can be determined from the measured frequency, the dimensions of the specimen, the Young's moduli of all the other layers, and the mass of the specimen. Generally, in the case of the TBC system specimen, the Young's modulus and thickness of the TC are approximately one order of magnitude lower than those of the substrate. Consequently, the modulus of a TC for a TBC multilayered specimen is considerably sensitive to experimental errors. This causes a large error in the obtained Young's modulus. The sensitivities of the method to input errors were investigated analytically as follows. Assuming a typical TBC system specimen, $E_s = 190$ GPa, $E_b = 110$ GPa, $E_c = 25$ GPa, $h_s = 2$ mm, $h_b = 0.1$, $h_c = 0.2$-0.7 mm, $L = 90$ mm, $b = 10$ mm, $\rho_s = 8{,}265$ kg/m^3, $\rho_b = 6{,}600$ kg/m^3, and $\rho_c = 5{,}405$ kg/m^3 were the input values used in the calculations. Here, the densities were used for evaluating the mass m. Figure 3 shows the ratio of Young's moduli calculated with and without error introduced into a particular input parameter. If the ratio is close to 1.0, the method can be considered insensitive to the input error. The horizontal axis in Fig. 3 denotes the relative thickness of the objective coating normalized by the substrate thickness, including the thickness of the BC for the TBC system specimen. The sensitivity of the BC system specimen for the Young's modulus of the BC is also plotted in Fig. 3. The calculation conditions were the same as the TBC system specimen except for $h_b = 0.1$-0.5 mm. Additionally, the sensitivities of four-point bending (4 PB) (Ref 9), which are the methods using the (i) load-coating strain, (ii) load-substrate strain, (iii) coating-substrate strain, and (iv) load-deflection are plotted.

Figure 3(a) shows the sensitivity to the error of the measured frequency f. An error of only +1% was input in the case of Fig. 3(a). Figure 3(a) shows that the resonance method is the most sensitive to the error as compared with the 4 PB methods; an error of +1% causes a large error in the obtained Young's modulus. However, the measured resonance frequency barely exhibited any error, because an error due to the measurement system generally does not significantly superpose on the resonance frequency. It will be understood from section 4.4 of experimental Young's modulus, which did not depend on the coating thickness. Figure 3(a) shows that a higher relative thickness of the coating causes greater insensitivity to the error; this was true for the other errors shown in Fig. 3(b)-(f). Finally, the Young's modulus of the TC was far more sensitive to the errors than that of the BC. This is because the effect of the TC on the resonance frequency of the coating system specimen was far lower than that of the BC owing to the lower TC Young's modulus. It was confirmed that the accuracy decreased if the Young's modulus of the objective coating was lower.

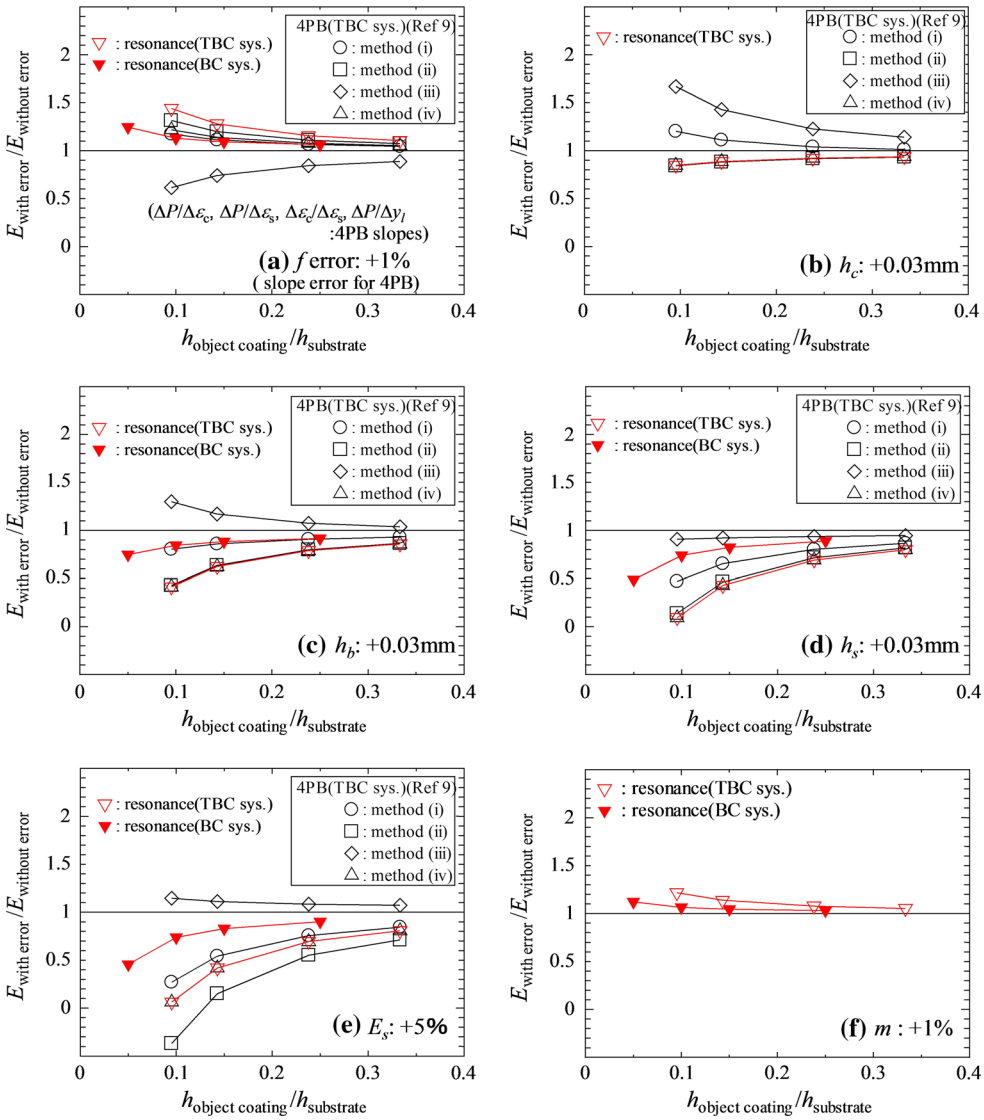

Fig. 3 The ratio of Young's moduli calculated with and without error introduced to a particular input parameter. If the ratio is close to 1.0, the method can be considered insensitive to the error. The horizontal axis denotes the relative thickness of the objective coating normalized by the substrate thickness, including the BC thickness for the TBC system specimen. (a) Sensitivity to the error in the frequency, (b) sensitivity to the error in the TC thickness, (c) sensitivity to the error in the BC thickness, (d) sensitivity to the error in the substrate thickness, (e) sensitivity to the error in the Young's modulus of the substrate, and (f) sensitivity to the error in the mass. The sensitivities of four-point bending (4 PB), which are the methods using the (i) load-coating strain, (ii) load-substrate strain, (iii) coating-substrate strain, and (iv) load-deflection are also plotted

Figure 3(b) and (c) show the sensitivity to the error in the thickness of the TC and BC (h_c and h_b), respectively. For thermal spray coatings, both the surface roughness and the interfacial roughness are high, and coating-thickness errors, h_c and h_b, are inevitable. As shown in Fig. 3(b) and (c), an error of +0.03 mm was input. Figure 3(b) and (c) show that the resonance method was sensitive to the error in the BC thickness and insensitive to the error in the TC thickness. The effective thickness (mean thickness of rough interface/surface), should be accurately measured by an image analysis of the longitudinal section, and not by the apparent thickness using a micrometer.

The resonance frequency of a TBC system specimen is mainly determined by that of the substrate because the thickness and Young's modulus of the substrate are approximately one order of magnitude higher than those of the TC. Figure 3(d) and (e) shows the sensitivity to the errors of the substrate thickness and substrate modulus (h_s and E_s), respectively. As shown in Fig. 3(d) and (e), a thickness error of +0.03 mm and a modulus error of +5% were input, respectively. For example, in Fig. 3(d) and (e), there is a case where the estimated E_c becomes near zero. Because the resonance frequency of the specimen was mainly determined by that of the substrate, a small $+h_s$ or

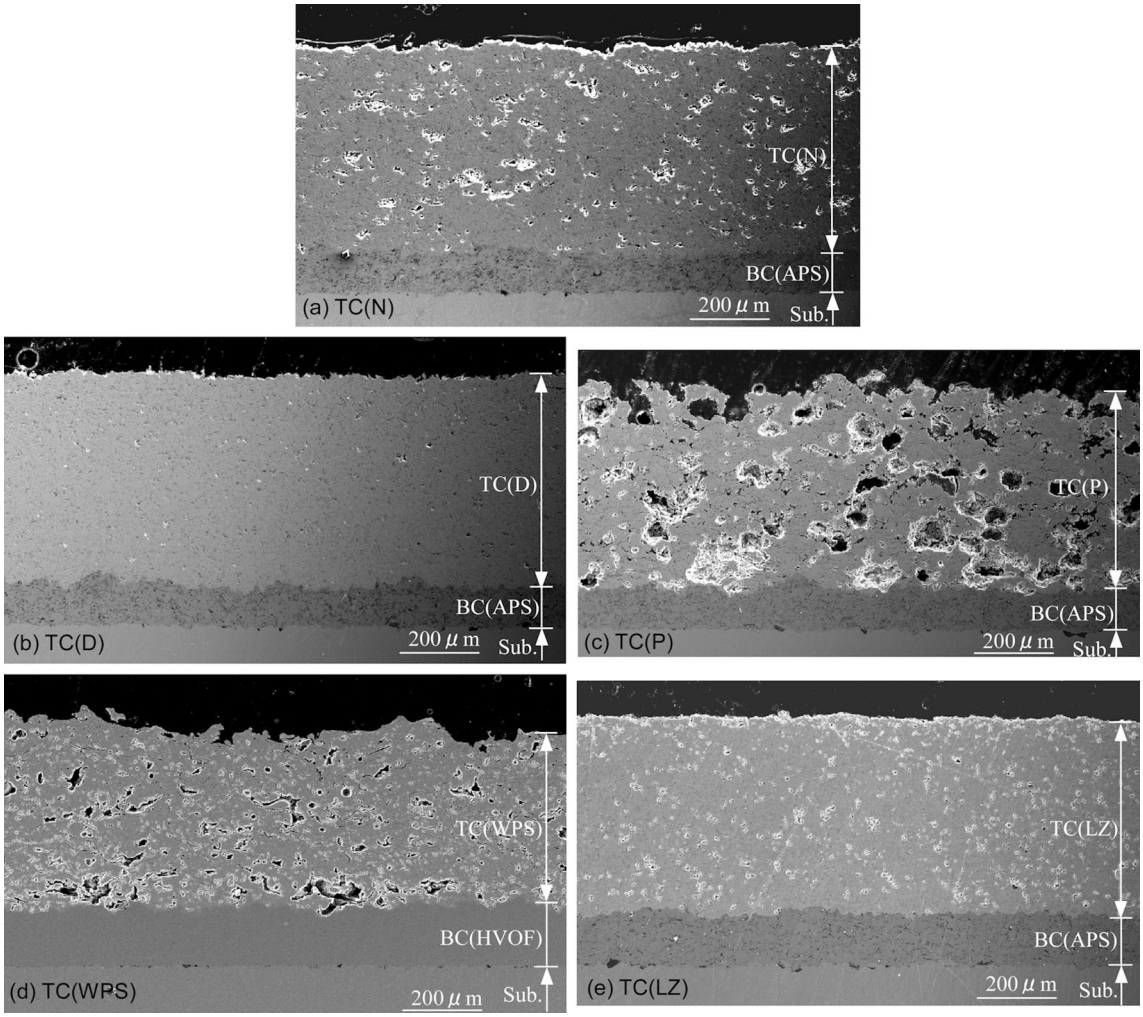

Fig. 4 Images of longitudinal sections of the TBC system specimens obtained using SEM (Ref 9). (a) TC(N), (b) TC(D), (c) TC(P), (d) TC(WPS), and (e) TC(LZ)

$+E_s$ error causes a significant change in E_c. This confirms that the values of the substrate are important for accurately measuring the Young's modulus of the TC using the composite-beam specimen similar to 4 PB tests. Fortunately, these values of the substrate can be measured accurately because the substrate roughness is far lower than that of a sprayed surface, and the modulus of the substrate can be also determined accurately because the substrate is not a multilayered specimen.

Finally, Fig. 3(f) shows the affection of mass error, +1%. The magnitude of the affection is insignificant. The affections of the other input errors, i.e., the width b, length L, and modulus E_b, were relatively insignificant similar to 4 PB tests. However, in the case of thermal expansion that leads to a significant change in the dimensions of the substrate, if the temperature change is large, the error causes a large error in the obtained Young's modulus. Therefore, the change in the dimensions should be included in the input values for evaluating the Young's modulus at high temperature.

4. Experimental Verification

4.1 TBC System Specimen

The substrate used in this study was a Ni-base superalloy (Hastelloy X), one side of which was blasted. Subsequently, the BC and TC were deposited on the substrate by atmospheric plasma spraying (APS). The BC and TC were made of CoNiCrAlY (Co-32Ni-21Cr-8Al-0.5Y, AMDRY9954 powder) and YSZ (ZrO_2-$8Y_2O_3$, Metco204NS powder), respectively. The YSZ TC is called the TC(N) herein. A dense YSZ (ZrO_2-$6Y_2O_3$, ShowaK-89 powder) coating and a porous YSZ (ZrO_2-$8Y_2O_3$, Metco204NS-G + 10% Polyester powder) coating were also manufactured by APS; these are called the TC(D) and TC(P), respectively. A water plasma-sprayed (WPS) YSZ (ZrO_2-$8Y_2O_3$, Metco204NS powder) coating and a $La_2Zr_2O_7$ (powder particle size: 10-44 μm) coating by APS were also fabricated; these are called the TC(WPS) and TC(LZ), respectively. The BC of the TC(WPS) sys-

tem specimen was deposited by high-velocity-oxy-fuel (HVOF) spraying. Scanning electron microscope (SEM, JEOL JSM-6510LA) images of these five specimens are shown in Fig. 4. The specimens are identical to those reported in a previous work of 4 PB (Ref 9).

Four TC(N)s with different thicknesses were prepared; thus, they exhibited four levels of sensitivities. The apparent dimensions of the specimens, determined through micrometer measurements, are listed in Table 1. For example, the thickness of the BC was determined by subtracting the thickness of the substrate from the total thickness after the deposition of the BC. There were two specimens for each thickness in Table 1. The thicknesses used in calculations were actual values measured with 1 μm resolution for the individual specimens. The effective thickness (mean thickness of rough interface/surface) was evaluated by an image analysis of the longitudinal section. The length of the specimens L was 90 mm, and the width b was 10 mm. The side surfaces of the specimens were polished to remove the coating deposited on them while the surfaces of the coatings were in the as-sprayed condition.

Table 1 Apparent thickness of the TBC system specimens used in this study (mm)

Code	Substrate (Hastelloy X)	BC (CoNiCrAlY)	TC
TC (N)	2.05	0.15	0.21
	2.05	0.15	0.32
	2.05	0.15	0.52
	2.04	0.15	0.69
TC (D)	2.05	0.14	0.52
TC (P)	2.06	0.15	0.50
TC (WPS)	2.05	0.17	0.49
TC (LZ)	2.05	0.17	0.49

4.2 Experimental Procedure

The resonance method with mode identification by a needle tripod and laser Doppler interferometer (LDI) was originally developed for resonance ultrasound spectroscopy of a small sample by Ogi et al. (Ref 20). In this study, the resonance frequency was measured by the resonance device with a needle tripod as shown in Fig. 5. A specimen was placed on the needle tripod with no external force applied on it except for the specimen's weight. Piezoelectric transducers, functioning as a transmitter and receiver, were built into the left needle and one of the right needles. The other right needle was a support for the specimen's weight. These supports were located at the nodes of the first bending mode. The specimen was oscillated by the left piezoelectric transducer by a continuous sinusoidal signal, and the amplitude of oscillation was measured by the right piezoelectric transducer. Sweeping the oscillation frequency with a 1 Hz resolution and measuring the oscillation amplitude for a duration of 6 s at each frequency, the power spectrum as a function of frequency was evaluated. The resonance amplitude was small as will be shown in section 4.3, because the amplitude was detected at the node. However, the relative amplitudes around the resonance frequency became distinctly high and distinguishable from those of non-resonances.

The distribution of the out-of-plane displacement, which can determine the resonance mode, was identified by the LDI shown in Fig. 5, as the confirmation of the

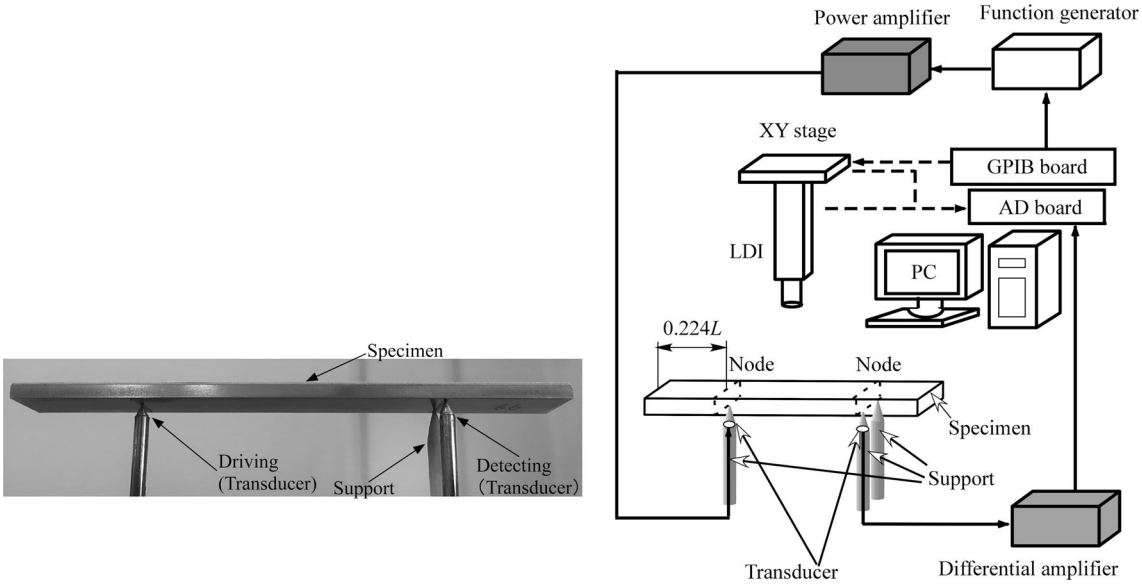

Fig. 5 Resonance device with a needle tripod and LDI. A specimen was placed on the needle tripod with no external force applied on it except for the specimen's weight. Piezoelectric transducers, functioning as a transmitter and receiver, were built into the left needle and one of the right needles. The other right needle was a support for the specimen's weight. The specimen was oscillated by the left transducer, and the amplitude of oscillation was measured by the right transducer. Sweeping the oscillation frequency, the power spectrum as a function of frequency was evaluated. Resonance mode was identified by the displacement-distribution patterns measured by the LDI

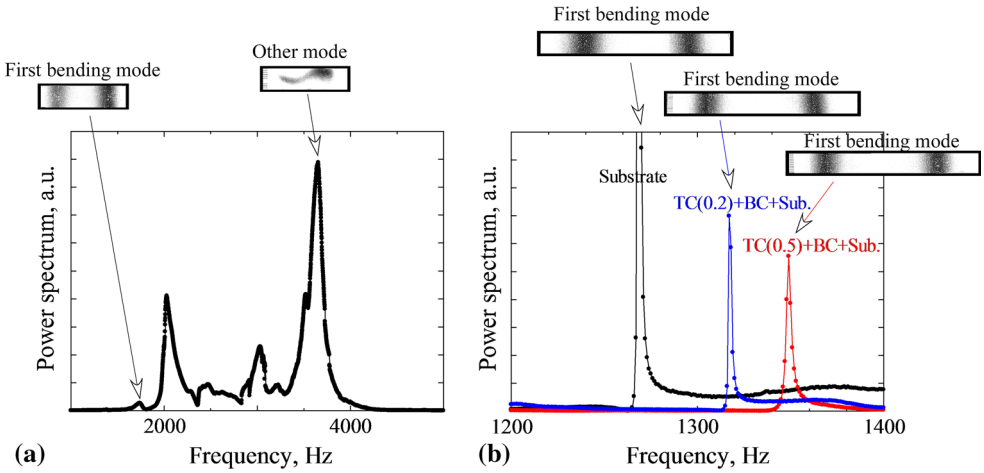

Fig. 6 Power spectrum plotted with respect to the oscillation frequency. Distributions of the specimen displacement was measured by the LDI. The black regions are node, and white regions are antinode. (a) Freestanding TC, (b) substrate, and TBC systems

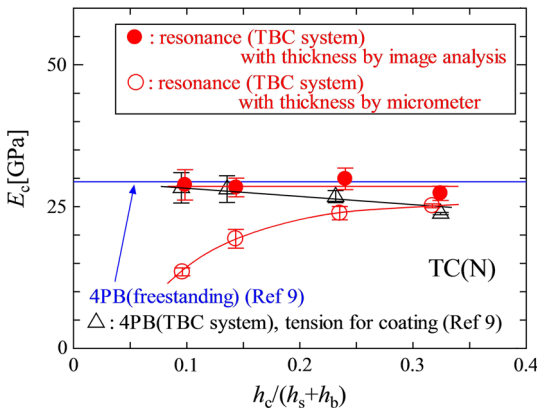

Fig. 7 Results for the Young's modulus of the TCs of different thickness measured on TBC system specimens

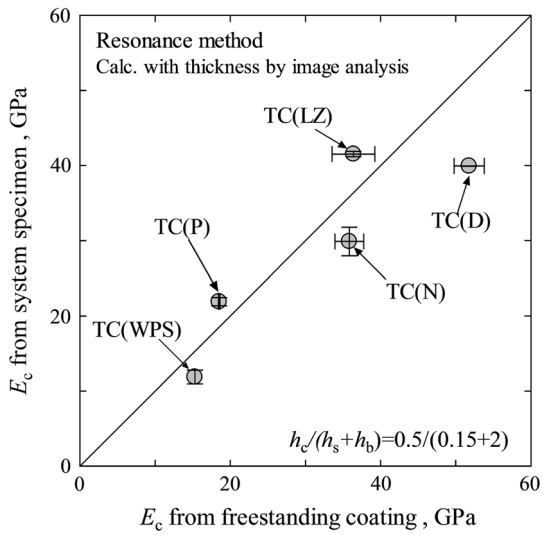

Fig. 8 Comparison of the Young's modulus, E_c, of various TCs between those obtained through the resonance of TBC system specimens and those through the resonance of freestanding specimens

resonance mode is very important in resonance methods. The first bending mode was determined from among the displacement-distribution patterns at the peak frequencies of the power spectrum. The peak frequency of first bending mode was adopted as the resonance frequency.

4.3 Resonance Frequency

Figure 6(a) and (b) plots the power spectrum with respect to the oscillation frequency for the freestanding TC(N) and TC(N) system specimens, respectively. The freestanding TC specimen exhibits a broad peak with significant internal friction. On the contrary, the TBC system specimen exhibits a sharp peak, because the resonance was almost determined by the substrate.

Figure 6(a) shows some peaks, and we cannot distinguish which one corresponds to the first bending resonance only from the amplitude of the peaks. The distributions of specimen displacement measured by the LDI are shown in Fig. 6(a). The black regions are node, and the white regions are antinode. In this case, 1741 Hz is the frequency of first bending resonance. The other peaks do not correspond to the first bending resonance. In the case of the resonance with tripod support at nodes, identifying the mode was important because the detected displacement at the node for the first bending resonance was much smaller than the other resonance modes, in which the measured point might be close to antinode.

On the other hand, Fig. 6(b) shows sharp resonance peaks of the TBC system specimens. In this figure, the peak of a substrate specimen without coatings is also shown. We find the peaks of the TBC system specimens near the peak of the substrate. This is because the frequency was almost determined by the substrate with a large E_s and h_s. The frequency of the first bending resonance on the substrate was previously known because the Young's modulus of the substrate is well known, which means that the peak of the first bending resonance of a

Table 2 Apparent thickness of the BC system specimens used in this study (mm)

Process	Substrate (Hastelloy X)	BC (CoNiCrAlY)	Heat treatment
APS	2.05	0.32	…
HVOF	2.07	0.31	…
HVOF	2.07	0.31	1373 K, 100 h in air

multilayered specimen is correctly determined by searching around the peak of the substrate without mode identification. This is a great advantage to determine the resonance mode of a multilayered specimen with certainty.

Finally, we discuss the amplitude of the specimens that will relate to the strain of the TC. The difference of amplitudes between the center of the specimen and node of the specimen were lower than approximately 5 nm for the multilayered specimens. Therefore, the strain ranges generated on the TC surface were small enough that inelastic effects could be neglected. Similarly to the multilayered specimen, the amplitudes in displacement of freestanding TCs were also small enough.

4.4 Young's Moduli of the TC with Several Thicknesses

The obtained Young's moduli of the TC(N) from the TBC system specimens with several thicknesses are shown in Fig. 7. For the calculations, we used $E_s = 195.7$ GPa for the substrate and $E_b = 100.6$ GPa for the BC. These values were determined from the resonance of the single-layer specimens. The mass of the specimen and dimensions of each layer in the TBC system specimens were measured and used in the calculation. There were two specimens for each thickness, and the error bar indicates the data range. In Fig. 7, the Young's moduli obtained by the bending methods for a freestanding specimen and TBC system specimens are shown. As described in section 3, the error of BC thickness significantly affects the obtained Young's modulus. Therefore, the results for both of the effective thicknesses, h_b and h_c, obtained by performing an image analysis from the longitudinal section and the apparent thicknesses using a micrometer are shown in Fig. 7. The horizontal axis of Fig. 7 indicates the relative thickness of the TC compared with that of the sum of the substrate and BC. According to Fig. 7, the Young's modulus obtained by the apparent thickness rapidly decreases when the relative thickness decreases.

On the other hand, the modulus obtained by the effective thickness maintains a constant value. According to the sensitivity analysis presented in section 3, the accuracy of Young's modulus decreases when the relative thickness of the coating decreases. However, the error induced was very small, because the value remains constant independent of the thickness, which corresponds with the sensitivity to the errors. Further, the obtained Young's modulus is approximately the same as that measured through the 4 PB method in which the applied surface strain was 200 μstrain. In addition, the tensile modulus obtained through 4 PB was almost the same as the compressive modulus if determined by the most accurate 4 PB method using the load-coating strain (Ref 9).

4.5 Applications to TCs

In this section, for the calculation, we used the Young's moduli of the substrate and the BC(APS) that were described in section 4.4. Furthermore, $E_b = 118.0$ GPa for the BC(HVOF) was used for the calculations related to the TC(WPS) system specimens which BCs were deposited by HVOF spraying. The value was determined by the resonance using the freestanding specimen. The Young's moduli of the five types of TCs shown in Table 1 were determined using the resonance method of the TBC system specimen and shown in Fig. 8. There were two specimens for each material, and the error bar indicates the data range. In the calculation, the effective thicknesses obtained by the image analysis were used. The horizontal axis of Fig. 8 shows the Young's moduli determined by the resonance method for the freestanding specimens. There were two specimens except for the TC (WPS), and the error bar indicates the data range. The dimensions of the freestanding specimens were $L = 25$-60 mm, $b = 10$ mm, and $h_c = 1$ mm. The resonance modes of all the freestanding specimens were confirmed by the LDI, as shown in Fig. 5. For the TBC system specimens, the resonance frequency of first bending resonance appeared near that of the substrate as described in section 4.2. Figure 8 shows that the Young's modulus for the TBC system specimens was slightly higher or lower than those for the freestanding TC specimens, depending on the material. This dependency matches the comparison between the Young's moduli for the system specimens and those for the freestanding specimens through the 4 PB tests shown in Ref 9. Naturally, the property of the TC in a multilayered specimen differs from that in a freestanding specimen because of the difference in the thermal history during the thermal spraying. It can be confirmed that the Young's moduli for a multilayered specimen are not significantly different

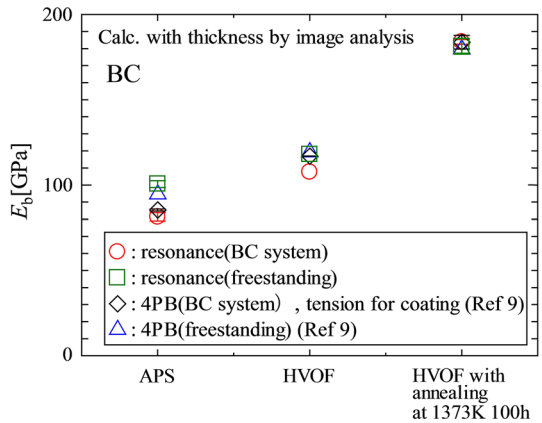

Fig. 9 Comparison of the Young's modulus, E_b, of various BCs between those obtained through the resonance of BC system specimens and the other methods

from those for a freestanding coating.

4.6 Applications to BCs

Table 2 presents the thicknesses of the BC system specimens, which comprised a BC and a substrate. The apparent thickness listed in Table 2 was determined using a micrometer. The length of the specimens L was 90 mm, and the width b was 10 mm. HVOF coatings thermally treated at 1373 K for 100 h in air were also prepared. Figure 9 shows the Young's moduli of the BCs obtained by the resonance method for the BC system specimens. In the calculation, the effective thicknesses by image analysis were used. For the calculations, we used $E_s = 195.7$ GPa for the substrate. Figure 9 also shows other results of the 4 PB method for the BC system and freestanding specimens in which the applied surface strains were 200 μstrain, and the resonance method for freestanding specimens. There were two specimens for the resonance method on BC systems and freestandings except for the HVOF (as spray) specimen, and the error bar indicates the data range. The dimensions of the freestanding specimens were $L = 50$ mm, $b = 10$ mm, and $h_b = 1$ mm. There is a slight difference in the Young's modulus for BC(APS) and BC(HVOF) but little difference for the BC(HVOF with annealing) with high E_b. It can be confirmed that the BC moduli from a multilayered specimen are not significantly different from those obtained by other methods similar to the results of TCs shown in section 4.5.

5. Conclusions

We developed an evaluation method for the Young's modulus of the TBC layer based on the first bending resonance of a TBC system specimen. First, we derived a closed-form solution for the Young's modulus of the TBC layer using the TBC system specimen. Next, we performed a sensitivity analysis of the input errors to reveal the important inputs for accurate evaluation. Finally, we experimentally investigated the accuracy for some typical TBCs and demonstrated the effectiveness of the proposed method.

(1) We derived the closed-form solution for the Young's modulus of the TBC layer using the equation of the motion for the bending vibration of a three-layered composite beam. The solution provides the Young's modulus of the TBC layer using the measured resonance frequency and known values such as the dimensions, mass, and Young's moduli of all the other layers.

(2) In the case of the TBC system specimen, the Young's modulus and thickness of the TBC layer are generally approximately one order of magnitude lower than those of the substrate. Consequently, the modulus of a TBC layer determined from a multilayered specimen is considerably sensitive to experimental errors. This causes a large error in the obtained Young's modulus. According to the analysis of the sensitivity to errors, the Young's modulus and thickness of the substrate are very important inputs for accurately determining the Young's modulus of TBC layer. The measured frequency and thickness of the BC are secondarily important.

(3) The frequency of the first bending resonance on the substrate was previously known because the Young's modulus of the substrate is well known. Thus, the peak of the first bending resonance of a multilayered specimen is certainly determined by searching around the peak of the substrate without mode identification. This is a great advantage for determining the resonance mode of a multilayered specimen with certainty.

(4) The experimental verification confirmed that the resonance method of a TBC multilayered specimen provides a reasonable Young's modulus as compared with other methods.

Acknowledgment

We wish to thank Prof. H. Ogi (Osaka University) for useful advice on the resonance device, and also thank Dr. Y. Kojima (Hitachi, Ltd., retired) and Mr. F. Ono (Osaka Science & Technology Center) for useful advice on specimens. This research was financially supported by the Ministry of Economy, Trade and Industry (METI) of Japan.

References

1. U. Schulz, K. Fritscher, and M. Peters, EB-PVD Y_2O_3-and CeO_2/Y_2O_3-Stabilized Zirconia Thermal Barrier Coatings—Crystal Habit and Phase Composition, *Surf. Coat. Technol.*, 1996, **82**(3), p 259-269
2. C.A. Johnson, J.A. Ruud, R. Bruce, and D. Wortman, Relationships Between Residual Stress, Microstructure and Mechanical Properties of Electron Beam-Physical Vapor Deposition Thermal Barrier Coatings, *Surf. Coat. Technol.*, 1998, **108-109**, p 80-85
3. H.B. Guo, R. Vaßen, and D. Stöver, Atmospheric Plasma Sprayed Thick Thermal Barrier Coatings with High Segmentation Crack Density, *Surf. Coat. Technol.*, 2004, **186**(3), p 353-363
4. H.B. Guo, S. Kuroda, and H. Murakami, Segmented Thermal Barrier Coatings Produced by Atmospheric Plasma Spraying Hollow Powders, *Thin Solid Films*, 2006, **506-507**, p 136-139
5. K.V. Niessen and M. Gindrat, Plasma Spray-PVD: A New Thermal Spray Process to Deposit Out of the Vapor Phase, *J. Therm. Spray Technol.*, 2011, **20**(4), p 736-743
6. N.P. Padture, K.W. Schlichting, T. Bhatia, P. Miranzo, and M.I. Osendi, Towards Durable Thermal Barrier Coatings with Novel Microstructures Deposited by Solution-Precursor Plasma Spray, *Acta Mater.*, 2001, **49**(12), p 2251-2257
7. M. Beghini, G. Benamati, L. Bertini, and F. Frendo, Measurement of Coating's Elastic Properties by Mechanical Methods: Part 2. Application to Thermal Barrier Coatings, *Exp. Mech.*, 2001, **41**(4), p 305-311
8. H. Waki, H. Fujioka, Y. Harada, M. Okazaki, and A. Kawasaki, Young's Modulus of Thermal Barrier Coating and Oxidation Resistant Coating Bonded to Stainless Substrate by Four-Point Bending, *J. Solid Mech. Mater. Eng.*, 2010, **4**(2), p 274-285
9. H. Waki, A. Oikawa, M. Kato, S. Takahashi, Y. Kojima, and F. Ono, Evaluation of the Accuracy of Young's Moduli of Thermal Barrier Coatings Determined on the Basis of Composite Beam Theory, *J. Therm. Spray Technol.*, 2014, **23**(8), p 1291-1301

10. E.F. Rybicki, J.R. Shadley, Y. Xiong, and D.J. Greving, Cantilever Beam Method for Evaluating Young's Modulus and Poisson's Ratio of Thermal Spray Coatings, *J. Therm. Spray Technol.*, 1995, **4**(4), p 377-383
11. A. Kucuk, C.C. Berndt, U. Senturk, R.A. Lima, and C.R.C. Lima, Influence of Plasma Spray Parameters on Mechanical Properties of Yttria Stabilized Zirconia Coatings. I: Four Point Bend Test, *Mater. Sci. Eng., A*, 2000, **284**(1-2), p 29-40
12. M. Hasegawa and Y. Kagawa, Microstructural and Mechanical Properties Changes of a NiCoCrAlY Bond Coat with Heat Exposure Time in Air Plasma-Sprayed Y_2O_3-ZrO_2 TBC systems, *Int. J. Appl. Ceram. Technol.*, 2006, **3**, p 293-301
13. M. Matsumoto, K. Wada, N. Yamaguchi, T. Kato, and H. Matsubara, Effects of Substrate Rotation Speed during Deposition on the Thermal Cycle Life of Thermal Barrier Coatings Fabricated by Electron Beam Physical Vapor Deposition, *Surf. Coat. Technol.*, 2008, **202**(15), p 3507-3512
14. X.Q. Ma, Y. Mizutani, and M. Takemoto, Laser-Induced Surface Acoustic Waves for Evaluation of Elastic Stiffness of Plasma Sprayed Materials, *J. Mater. Sci.*, 2001, **36**, p 5633-5641
15. H.-L.R. Chen, B. Zhang, M.A. Alvin, and Y. Lin, Ultrasonic Detection of Delamination and Material Characterization of Thermal Barrier Coatings, *J. Therm. Spray Technol.*, 2012, **21**(6), p 1184-1194
16. M. Arai and K. Kishimoto, Estimation Method of Young's Modulus of Thermal Barrier Coating Layer Based on Free Bending Vibration, *J Soc. Mater. Sci. Jpn.*, 2003, **52**(9), p 1135-1139 ((in Japanese))
17. S. Patsias, N. Tassini, and K. Lambrinou, Ceramic Coatings: Effect of Deposition Method on Damping and Modulus of Elasticity for Yttria-Stabilized Zirconia, *Mater. Sci. Eng., A*, 2006, **442**(1-2), p 504-508
18. S. Timoshenko, D.H. Young, and W. Weaver, *Vibration Problems in Engineering Materials*, 4th ed., Wiley, New York, 1974, p 424
19. C.C. Chiu and E.D. Case, Elastic Modulus Determination of Coating Layers as Applied to Layered Ceramic Composites, *Mater. Eci. Eng. A*, 1991, **132**, p 39-47
20. H. Ogi, K. Sato, T. Asada, and M. Hirao, Complete Mode Identification for Resonance Ultrasound Spectroscopy, *J. Acoust. Soc. Am.*, 2002, **112**(6), p 2553-2557